Electronic Supplementary Material (ESI) for Chemical Communications.
This journal is © The Royal Society of Chemistry 2022
Electronic Supplementary Material (ESI) for Chemical Communications.
This journal is © The Royal Society of Chemistry 2022

# Supporting Information

# A mass-tagged MOF nanoprobe approach for ultra-sensitive protein quantification in tumor-educated platelets

Xiuyu Chen,[a] Jianhua Zhu,[a] Bo Sun,[a] Xian Zhang,[a] Yechen Hu,[*a] Yun Chen[*abc]

[a] School of Pharmacy, Nanjing Medical University, Nanjing, 211166, China

[b] State Key Laboratory of Reproductive Medicine, 210029, China

[c] Key Laboratory of Cardiovascular & Cerebrovascular Medicine, Nanjing, 211166, China

*Correspondence: Dr. Yun Chen and Dr. Yechen Hu, School of Pharmacy, Nanjing Medical University, 818 Tian Yuan East Road, Nanjing, 211166, China

E-mail: huyechen@njmu.edu.cn (Yechen Hu); ychen@njmu.edu.cn (Yun Chen)

Phone: 86-25-86868326

Fax: 86-25-86868467

# Table of Contents

approach.

## 3. Supplementary Tables

**Table S1.** List of the DNA sequences used in this study.

**Table S2.** Comparison of our approach with the previously reported signal amplification methods for CD44 quantification.

**Table S3.** Evaluation of the accuracy and precision of the mass-tagged MOF nanoprobe approach.

**Table S4.** Clinical information of normal individuals and breast cancer patients.

## 4. Supplementary Results

**4.1.** LC-MS/MS method of the mass tag.

**4.2.** Characterization results of the mass-tagged MOF nanoprobe.

**4.3.** Validation results of the mass-tagged MOF nanoprobe approach.

## 1. Supplementary Materials and Methods

### 1.1. Materials and instruments

Peptide mass tag (AVLGVDPFR) and the corresponding stable isotope-labeled internal standard were prepared by Synpeptide Co., Ltd. (Shanghai, China). All the DNA sequences including TA6 aptamer[1] and histidine magnetic beads were purchased from Sangon Biological Engineering Technology & Co. Ltd. (Shanghai, China). Zinc nitrate was purchased from Sinopharm Chemical Reagent Co., Ltd (Shanghai, China). 2-Methylimidazole was supplied by Sigma-Aldrich Inc. (St. Louis, MO, USA). Poly (ethylene glycol) (PEG, MW=2000 Da) was purchased from Ponsure Biological (Shanghai, China). Recombinant Human CD44 (C-6His), CD62P (PE anti-human) were purchased from Biolegend (San Diego, California, USA). Dulbecco's Modified Eagle Medium (DMEM), Roswell Park Memorial Institute (RPMI) 1640 medium, fetal bovine serum (FBS) and streptavidin-modified beads were obtained from Thermo Scientific (Logan, UT, USA). Trypsin was purchased from Promega (Madison, WI, USA). Phosphate buffered saline (PBS) was purchased from Beyotime Institute of Biotechnology (Haimen, China). Binding buffer (5 mmol/L $MgCl_2$, 4.5 g/L glucose, 0.1 g/L salmon sperm DNA, and 1 g/L BSA in PBS) was used to reduce the nonspecific binding of the activable aptamer. Acetonitrile (ACN) and methanol were HPLC grade and were purchased from Tedia Company, Inc. (Fairfield, OH, USA). Formic acid (FA) was purchased from Aladdin Chemistry Co., Ltd. (Shanghai, China). All the reaction solutions were treated with 0.1% diethylpyrocarbonate (DEPC) to inactivate nucleases.

Mass tag was analyzed by an AB SCIEX ExionLC AD system (AB SCIEX, Framingham, MA, USA) coupled with an AB SCIEX QTRAP 5500 mass spectrometry system (AB SCIEX, Framingham, MA, USA). An Agilent InfinityLab Poroshell 120 SB C18 column (2.7 μm, 30 mm × 2.1 mm, Agilent, USA) was used for LC separation. A F-4600 spectrofluorometer (Hitachi, Japan) was used to measure the $K_d$ for aptamer. The TEM images and the EDX elemental mapping were taken on JEM-2800 (JEOL, Japan). The size and zeta potential of particles were recorded on a Zs90 Zetasizer (Malvern, UK). SEM was conducted with a Zeiss Sigma 500 (Carl Zeiss AG, Germany).

FT-IR spectroscopy was performed on a Perkin Elmer Spectrum One Fourier Transformed Infrared spectrometer (Bruker Corporation, Germany). PXRD was recorded on a D8 Advance X-ray diffractometer (Bruker Corporation, Germany). An Aria III FACScan flow cytometer (Becton Dickinson, Franklin Lakes, NJ, USA) was used to assess the aptamer specificity. TGA analysis was performed on a Mettler TGA/DSC3+ (Mettler-Toledo, Switzerland).

**1.2. Preparation and characterization of the activable aptamer**

The activable aptamer was prepared by hybridization of the aptamer portion and the inhibitory DNA. First, 30 μL of 10 μM the aptamer portion and 45 μL of 10 μM inhibitory DNA were mixed, heated at 95 °C for 10 min, and slowly annealed by cooling to room temperature for approximately 60 min. Then, the mixture was hybridized at 37 °C for 60 min to form the activable aptamer. The obtained activable aptamer was stored at 4 °C for further use.

The binding affinity of activable aptamer was determined by incubating various concentrations of FITC-labeled activable aptamer with 100 μL of 500 nM histidine-tagged CD44 recombinant proteins for 60 min at 37 °C in the dark. After incubation, activable aptamer·CD44 complexes were immobilized on histidine magnetic beads for 90 min at 37 °C and then washed three times. Afterward, 100 μL of 500 nM competing DNA was added and the reaction was performed at 37 °C for 60 min in the dark. Finally, the supernatant was collected and the fluorescence was detected using a spectrofluorometer. The $K_d$ was calculated from the following equation:

$$Y = B_{max} X / (K_d + X) \quad (1)$$

where X is the concentration of the added activable aptamer, Y is the obtained fluorescence intensity and $B_{max}$ is the maximum binding capacity.

To test the specificity of the activable aptamer, MCF-7 cells (CD44-positive) and NIH-3T3 cells (CD44-negative) were separately collected in the exponential phase of growth. After washing three times with PBS, the cells were diluted to $1 \times 10^6$ cells/mL with binding buffer, and incubated with 45 μL of 10 μM FITC-labeled random DNA or FITC-labeled activable aptamer at 37 °C for 60 min in the dark. After

washing with PBS three times, 60 μL of 10 μM competing DNA was added into cells, which were incubated at 37 °C for an additional 60 min. Finally, the cells were centrifuged at 1000 rpm for 3 min, further washed at least three times with PBS, and resuspended in 500 μL of PBS for flow cytometric analysis.

### 1.3. Development and validation of liquid chromatography tandem mass spectrometry (LC-MS/MS) method

We used LC-MS/MS method to quantify mass tag. The mobile phase consisted of solvent A (water with 0.1% FA) and solvent B (100% ACN). An injection volume of 5 μL and a flow rate of 0.3 mL/min were used. Elution time of 10 min was performed for the mass tag samples with a gradient of 10% solvent B for 1 min, 10-90% solvent B for 4 min, 90-10% solvent B for 4 min, and 10% solvent B for 1 min. For mass spectrometry parameters, 550 °C ion source temperature and 5500 V ion spray voltage were used. The pressures of curtain gas, ion source Gas1, and ion source Gas2 were set to 35, 55, and 55 psi, respectively. The collision gas pressure was set to medium. All mass tags were scanned in positive electrospray ionization mode. Data were collected and analyzed using AB SCIEX Analyst software (version 1.6.3).

Furthermore, the calibration standards of CD44 were prepared by serially diluting the 1 mg/mL stock solutions into 10.0 pg/mL, 100 pg/ mL, 1.00 ng/mL, 10.0 ng/mL, and 100 ng/mL, respectively. Correspondingly, the QC standards (i.e., lower limit of quantification (LLOQ), low QC, mid QC, and high QC) were set at 10.0 pg/mL, 30.0 pg/mL, 1.00 ng/mL, 80.0 ng/mL.

### 1.4. Preparation of mass-tagged MOF nanoprobe

For ZIF-8 MOF preparation, 200 mg Zn $(NO_3)_2 \cdot 6H_2O$ was dissolved in 800 μL methanol, and 4 g 2-methylimidazole was dissolved in 8 mL methanol. Then, the 2-methylimidazole solution was added dropwise to the Zn $(NO_3)_2 \cdot 6H_2O$ solution dropwise and the mixture was stirred for 3 h at room temperature. The solvent was removed by centrifugation. The product was then washed three times with methanol and dried at 37 °C under vacuum.

For mass tag@ZIF-8 MOF preparation, first, 200 mg Zn $(NO_3)_2 \cdot 6H_2O$ was dissolved in 800 μL methanol, and 4 g 2-methylimidazole was dissolved in 8 mL methanol. Then, 10 μL mass tag solution (35 mg/mL) was mixed with the Zn $(NO_3)_2 \cdot 6H_2O$ solution with stirring. The 2-methylimidazole solution was further added and the mixture was stirred for 3 h at room temperature. The product was collected by centrifugation, followed by washing three times with methanol and drying at 37 °C under vacuum.

For PEG/mass tag@ZIF-8 MOF preparation, 40 mg $N_3$-PEG-$NH_2$ was dissolved in 4 mL deionized water. Then, the solution was dropped into 40 mg mass tag@ZIF-8 MOF, and the mixture was stirred at room temperature for 12 h. Finally, the product was collected by centrifugation, followed by washing three times with methanol and drying at 37 °C under vacuum.

For BDNA/PEG/mass tag@ZIF-8 MOF preparation, 15 mg PEG/mass tag@ZIF-8 MOF was dissolved in 1.5 mL deionized water, and then mixed with 30 μL of 100 μM binding DNA at 37 °C for 2 h. Then, the product was washed three times with methanol and dried at 37 °C under vacuum.

### 1.5. Acidic release of mass tag from the nanoprobe

The release experiment was performed by dissolving 0.1 mg BDNA/PEG/mass tag@ZIF-8 MOF into 1 mL PBS solution (pH 2.0 and 7.4) and ultrasonicated at 0 °C for 100 min. Then, the amount of released mass tag was detected by mass spectrometry.

The ultimate encapsulated number of the mass tag per BDNA/PEG/mass tag@ZIF-8 MOF particle (N) was calculated according to the following equation:

$$N = N_1 / N_2 = (N_3 - C_1V_1N_A) / N_2 \quad (2)$$

where $N_1$ is the encapsulated mass tag number in BDNA/PEG/mass tag@ZIF-8 MOF, $N_2$ is the number of BDNA/PEG/mass tag@ZIF-8 MOF particles, $N_3$ is the total number of mass tags added for preparation, $C_1$ is the concentration of the mass tag left after encapsulation, and $V_1$ is the reaction volume, $N_A = 6.02 \times 10^{23}$.

### 1.6. Cell culture and blood collection

MCF-7, NIH-3T3 and MDA-MB-231 cells were purchased from the Cell Resource Center of Chinese Academy of Medical Sciences. MCF-7 and NIH-3T3 cell lines were cultured in Dulbecco's Modified Eagle's Medium with 1% penicillin/streptomycin and 10% FBS, at 37 °C in a humidified incubator with 5% $CO_2$. MDA-MB-231 cells were fed in RPMI 1640 containing 10% FBS and 1% penicillin/streptomycin in a 37 °C incubator with 5% $CO_2$. Changing the culture medium every 2 days and then the exponential-phase cells were used in the subsequent experiments.

The collection of blood samples from breast cancer patients and normal individuals in this study was conducted in accordance with the guidelines approved by the Ethics Committee of Nanjing Medical University. Blood samples were collected from 54 breast cancer patients and 10 normal individuals at the Cancer Hospital of Jiangsu (Nanjing, China) between November 2020 and March 2021. Subjects with inflammatory disease, diabetes, or nonsteroidal anti-inflammatory drug use were excluded from the study. All the subjects received informed consent, and they were biologically unrelated and belonged to the Han ethnic group in Jiangsu Province, China.

### 1.7. Evaluation of the selectivity of the mass-tagged MOF nanoprobe approach

To test the selectivity of the mass-tagged MOF nanoprobe approach, a series of cell lines with differential expression of CD44, including MDA-MB-231 cells (high expression), MCF-7 cells (low expression), NIH-3T3 cells (negative), and MDA-MB-231 cells pretreated with CD44 antibody for blocking, were investigated. In blocking experiment, MDA-MB-231 cells were collected and pretreated with CD44 antibody (100 μg/mL) at 37 °C for 60 min. Afterwards, all the cells were incubated with 30 μL of 10 μM activable aptamer for 60 min at 37 °C. After washing with PBS three times, 60 μL of 10 μM competing DNA was added and incubated for an additional 60 min at 37 °C. Then, the supernatant was collected and incubated with 20 μL streptavidin-modified beads at 37 °C for 90 min with continuous shaking. After washing with PBS three times, the supernatant was discarded and the sediment was further incubated

with 200 μL BDNA/PEG/mass tag@ZIF-8 MOF (1 mg/mL) at 37 °C for 90 min. After washing with PBS three times, 200 μL PBS (pH 2.0) was added into the sediment and then treated with ultrasound at 0 °C for 20 min. Finally, after washing with 200 μL PBS (pH 2.0) three times, all the supernatants were combined and subjected to mass spectrometry.

**1.8. Platelet separation**

First, the whole blood samples were gently reversed and mixed several times, then centrifuged for 20 min at 120 ×g at room temperature to acquire the platelet-rich plasma within 24 h. Then, carefully drain the upper layer of platelet-rich plasma into a new tube, after which centrifuged for 20 min at 360 ×g at room temperature to obtain the platelets deposition. Finally, the platelets deposition was gently resuspended and washed with PBS at least three times for the following experiment.

To assess sample purity, seven lots of platelets were randomly selected and fixed in 3.7% (w/v) paraformaldehyde (PFA) for 20 min and stained with crystal violet at room temperature for another 20 min in the dark. Counts of nucleated cell were determined by manual cell counting on a microscope by two observers. Contamination was controlled in 1-5 nucleated cells per 10 million platelets. Furthermore, to assess blood platelet activation during platelets isolation, we measured the expression level of the platelet activation dependent marker P-selectin (CD62P). For flow cytometric analysis, the extracted platelets were prefixed in 0.5% formaldehyde, stained by PE-modified CD62P for 30 min in the dark, and stored in 1.0% formaldehyde.

**1.9. Detection of CD44 protein in samples**

First, 30 μL of 10 μM activable aptamer was incubated with samples, including recombinant human CD44 protein (0.01-100 ng), breast cancer cells ($10^6$ cells) and extracted platelets (4 mL whole blood), for 60 min at 37 °C. After washing with PBS three times, 60 μL of 10 μM competing DNA was added and incubated for an additional 60 min at 37 °C. Then, the supernatant was collected and incubated with

20 μL streptavidin-modified beads at 37 °C for 90 min with continuous shaking. After washing with PBS three times, the supernatant was discarded and the sediment was further incubated with 200 μL BDNA/PEG/mass tag@ZIF-8 MOF (1 mg/mL) at 37 °C for 90 min. After washing with PBS three times, 200 μL PBS (pH 2.0) was added into the sediment and then treated with ultrasound at 0 °C for 20 min. Finally, after washing with 200 μL PBS (pH 2.0) three times, all the supernatants were combined and subjected to mass spectrometry.

## 2. Supplementary Figures

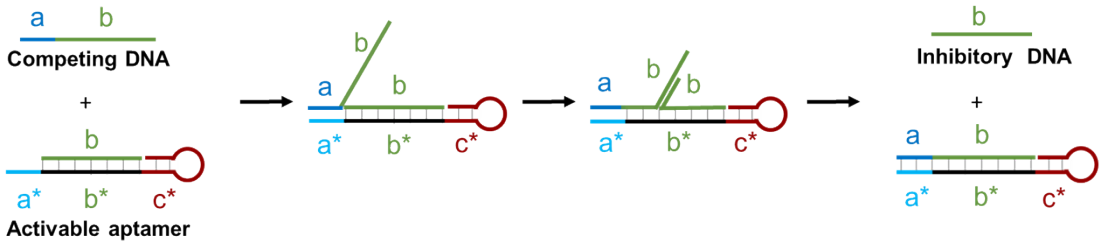


b: Inhibitory DNA  a + b: Competing DNA  a* + b* + c*: Aptamer portion

a*: Toehold domain  a* + b*: Extended sequence  c*: CD44 aptamer alone

**Figure S1.** Schematic illustration of toe-hold strand-displacement reaction (TSDR). TSDR is initiated by the hybridization of the competing DNA (a + b) with the toehold domain (a*) in the activable aptamer, and the inhibitory DNA (b) originally bound with the aptamer portion is subsequently released.

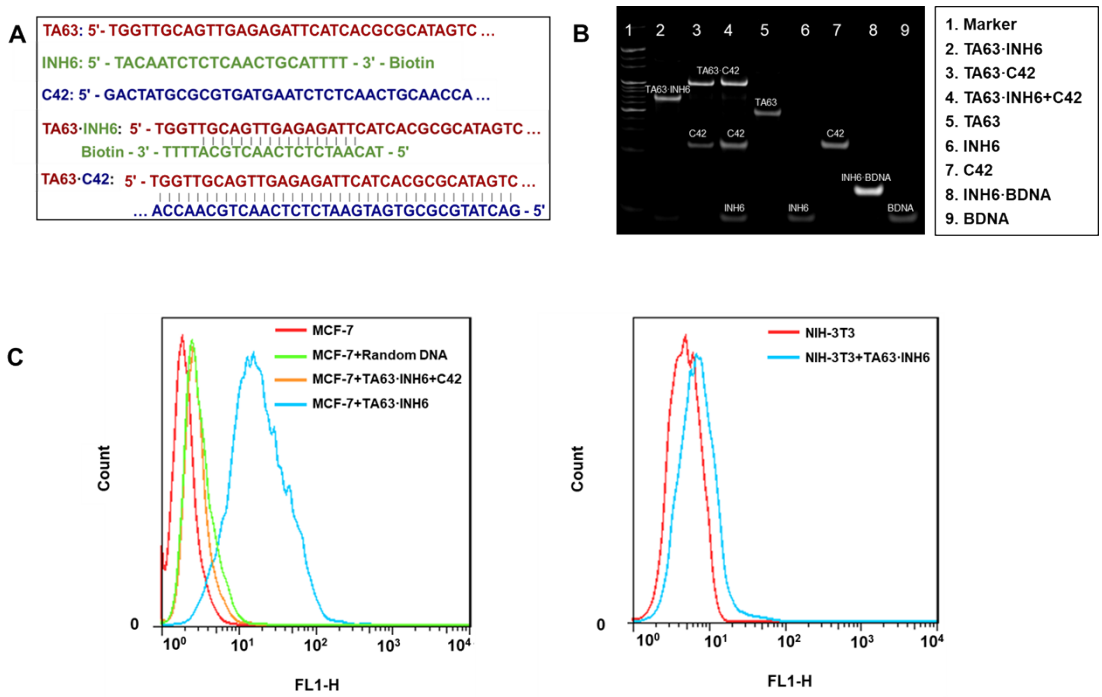


259

260 **Figure S2.** Characteristic evaluation of the activable aptamer. (A) Sequences of TA63,
261 the INH6 and C42 in the activable aptamer. Sequences of TA63·INH6 and TA63·C42
262 hybrids are also shown. (B) PAGE image of TA63, INH6 and C42 in the activable
263 aptamer, the BDNA in the mass-tagged MOF nanoprobe, and their corresponding
264 hybrids. (C) Flow cytometric analysis of MCF-7 cells and NIH-3T3 cells treated with
265 FITC-labeled activable aptamer and the FITC-labeled random DNA.

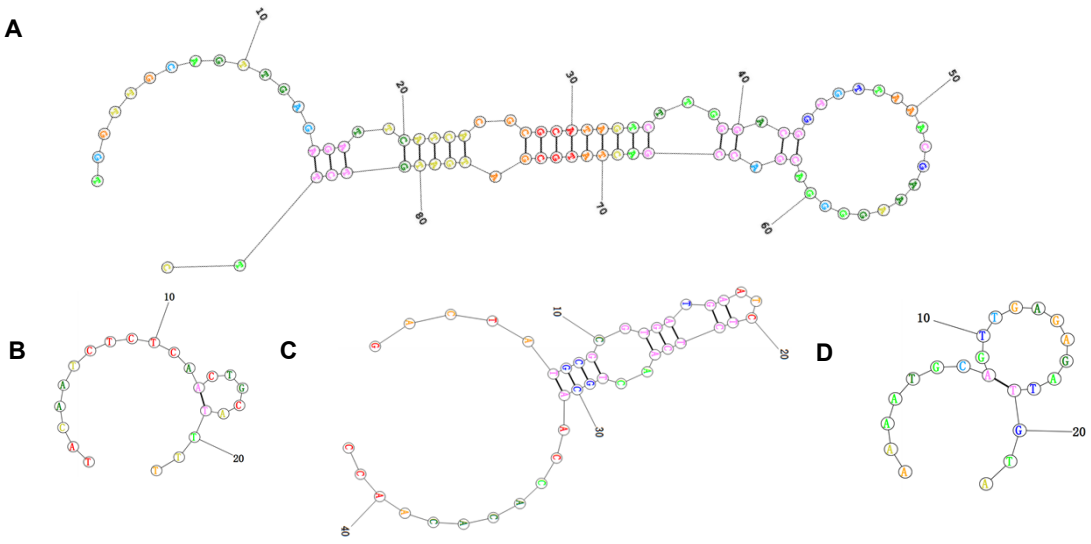


**Figure S3.** The secondary structures of (A) TA63, (B) INH6, (C) C42 and (D) BDNA were predicted using the RNAstructure software (http://rna.urmc.rochester.edu/RNA structureWeb/).

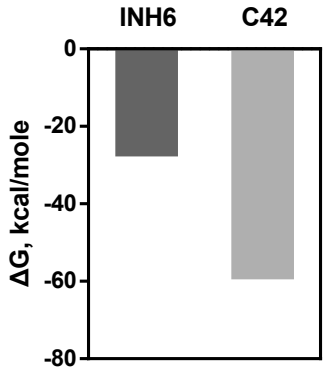


**Figure S4.** The ΔG values of the hybridization of INH6 and C42 with TA63 were predicted through an Oligo Analyzer analysis software (https://sg.idtdna.com/pages/tools/oligoanalyzer?returnurl=%2Fcalc%2Fanalyzer).

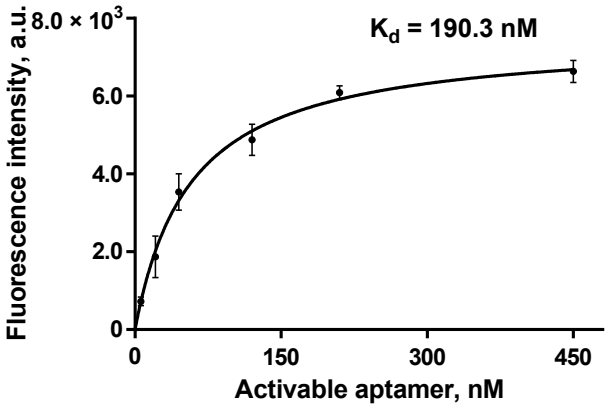


**Figure S5.** The representative binding curve of the activable aptamer with recombinant CD44 protein. Error bars represent the standard deviations of three replicate measurements.

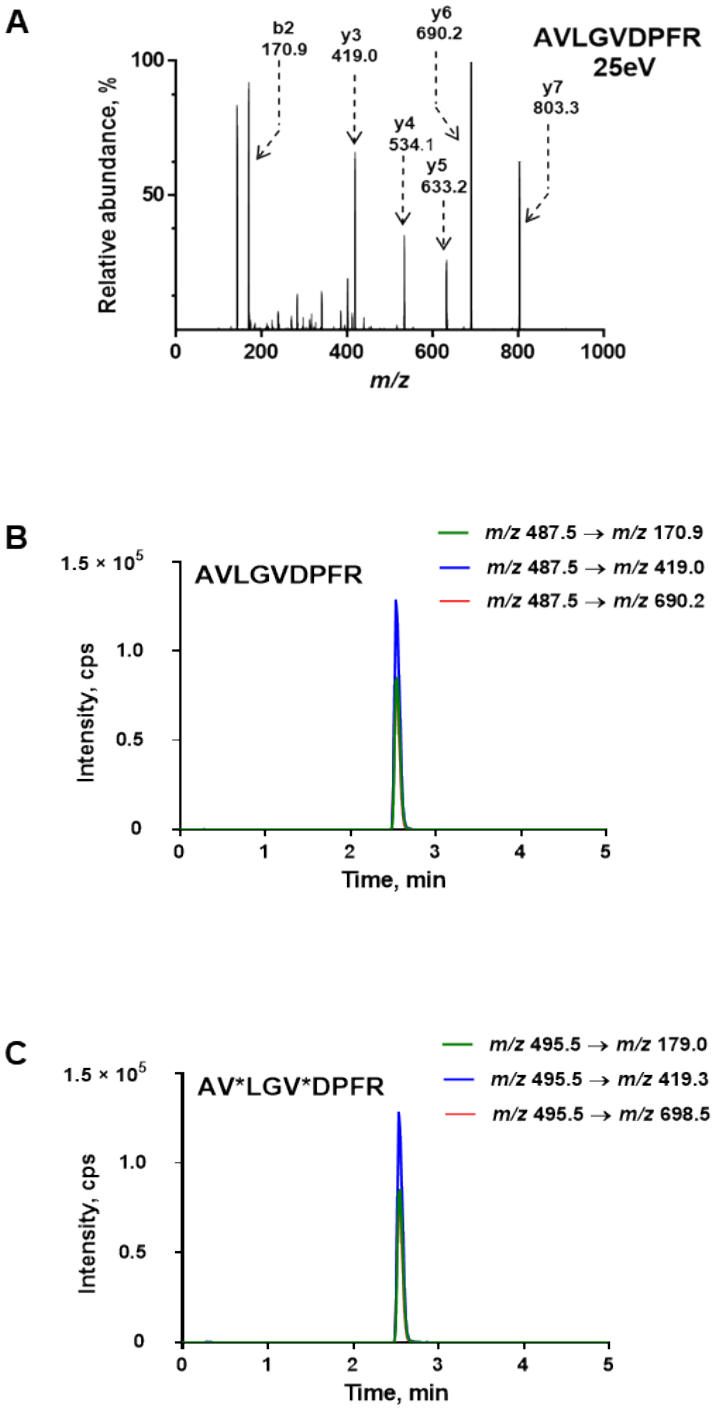


278

279 **Figure S6.** Establishment of mass spectrometry quantification method for the mass
280 tag. (A) The product ion spectrum of AVLGVDPFR, and (B-C) the LC-MS/MS
281 chromatograms of AVLGVDPFR and its corresponding isotope-labeled internal
282 standard AV*LGV*DPFR.

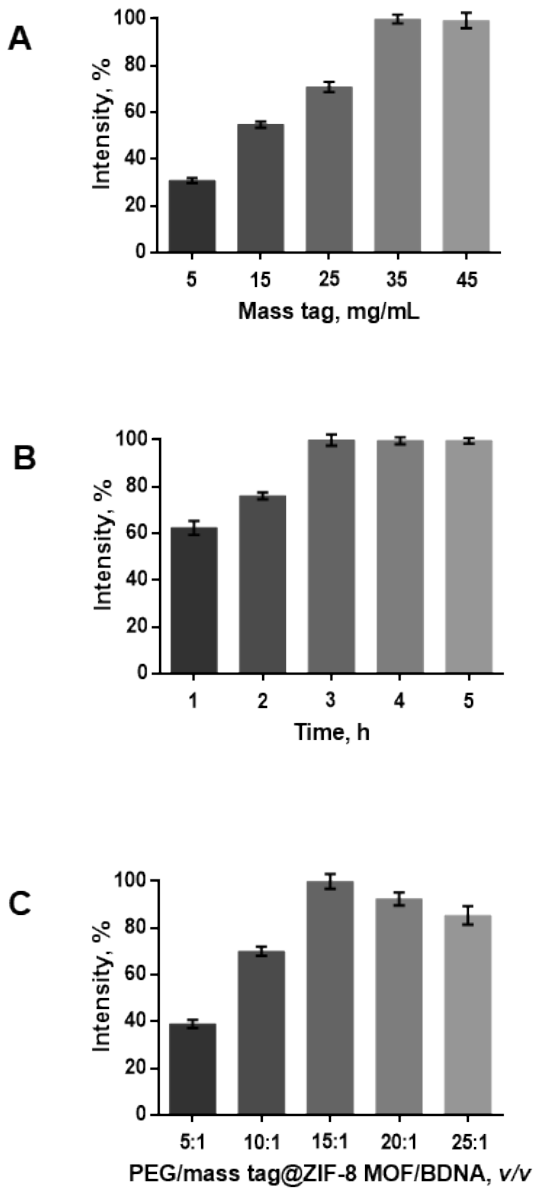


**Figure S7.** Optimization of the mass-tagged MOF nanoprobe preparation conditions, including (A) incubation concentration of the mass tag and (B) incubation time for the self-assembly reaction, and (C) reaction ratio of PEG/mass tag@ZIF-8 MOF and BDNA *via* copper-free click reaction. The incubation concentration of the mass tag ranged from 5 mg/mL to 45 mg/mL while keeping the reaction time of 2 h. Reaction time varied in the range of 1 h to 5 h with the incubation concentration of the mass tag as 35 mg/mL. Reaction ratio of PEG/mass tag@ZIF-8 MOF and BDNA (1 μM) ranged from 5:1 to 25:1. Error bars represent the standard deviations of three replicate measurements.

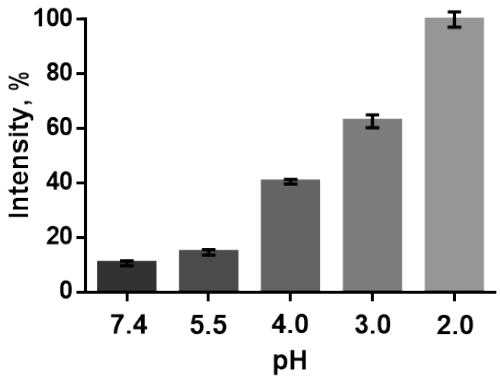


**Figure S8.** pH effect on acidolysis of the mass-tagged MOF nanoprobe. pH of acidolysis varied between 2.0 and 7.4. Error bars represent the standard deviations of three replicate measurements.

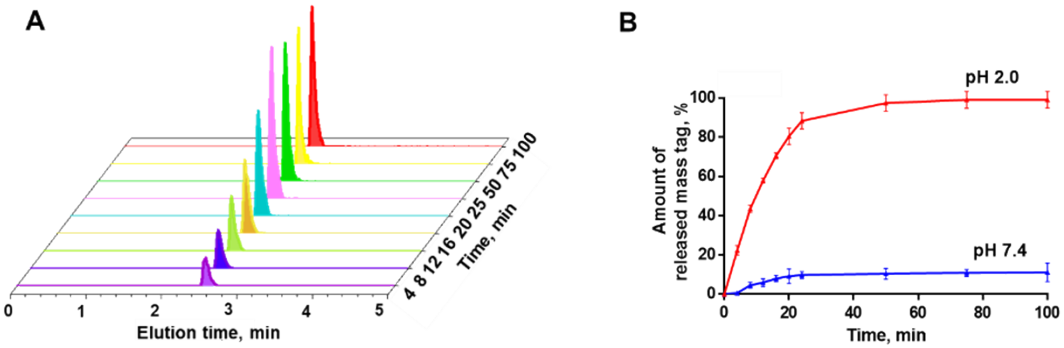


**Figure S9.** Characteristic evaluation of the mass tag. (A) Signal of the mass tag released from BDNA/PEG/mass tag@ZIF-8 MOF after different acidolysis times at pH 2.0. (B) Cumulative curves of the mass tag released from the BDNA/PEG/mass tag@ZIF-8 MOF at pH 7.4 and pH 2.0. Error bars represent the standard deviations of three replicate measurements.

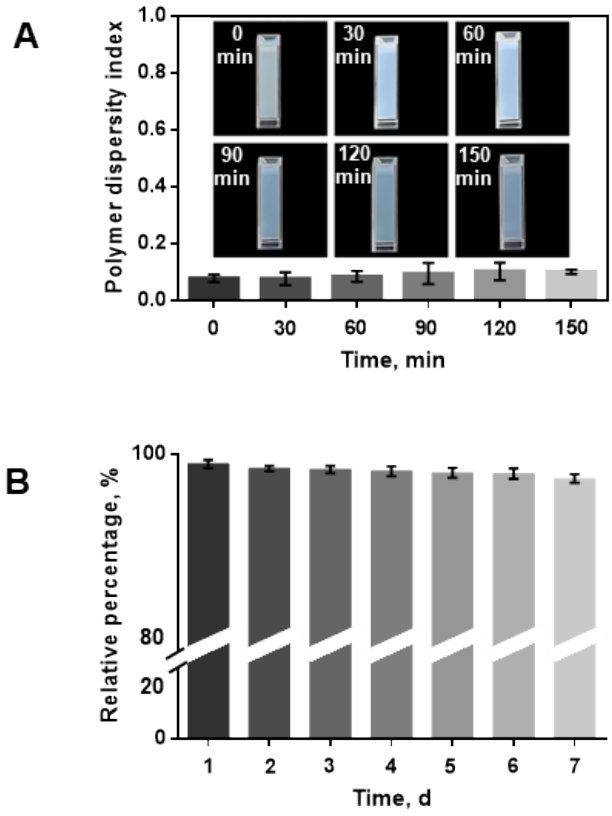


**Figure S10.** Dispersibility and stability of the mass-tagged MOF nanoprobe. (A) PDI of the nanoprobe at room temperature after the time period ranging from 0 to 150 min. (B) The mass spectrometric signals detected using the nanoprobe through a week. Error bars represent the standard deviations of three replicate measurements.

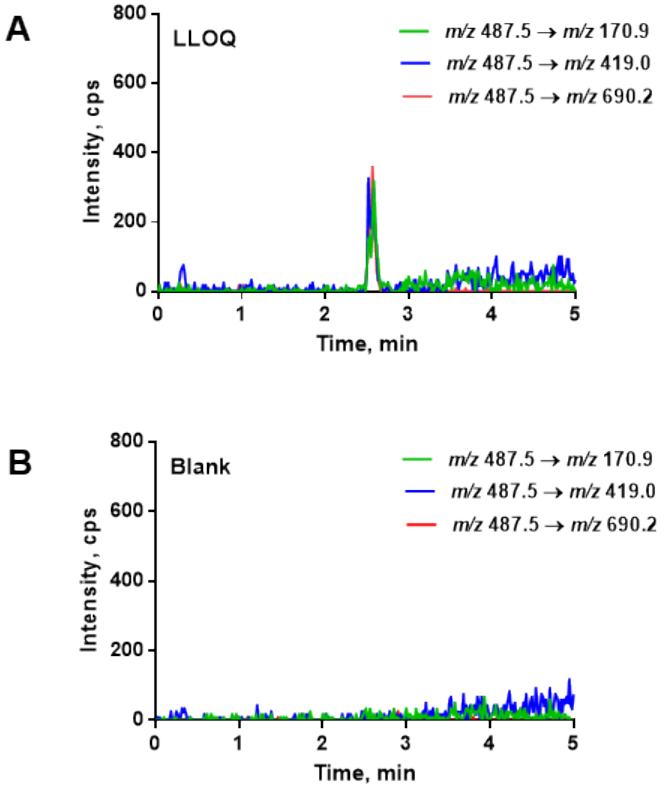


308

309 **Figure S11.** LC-MS/MS chromatograms of (A) LLOQ and (B) matrix blank.

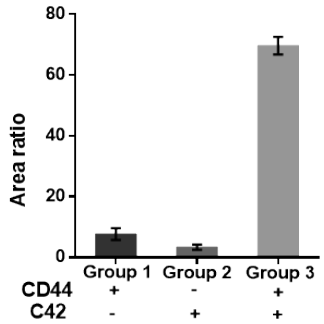


**Figure S12.** Selectivity of the mass-tagged MOF nanoprobe approach. No significant signal was detected in the absence of CD44 or C42.

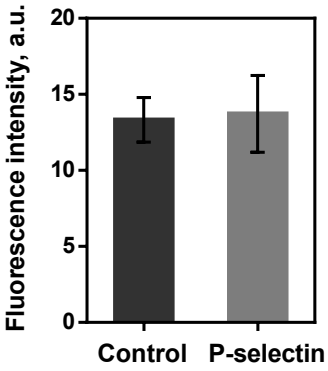


**Figure S13.** Measurement of P-selectin expression as the platelet activation marker in normal individuals and controls. Controls are the platelets that were not incubated with PE-modified P-selectin. Error bars represent the standard deviations of three replicate measurements.

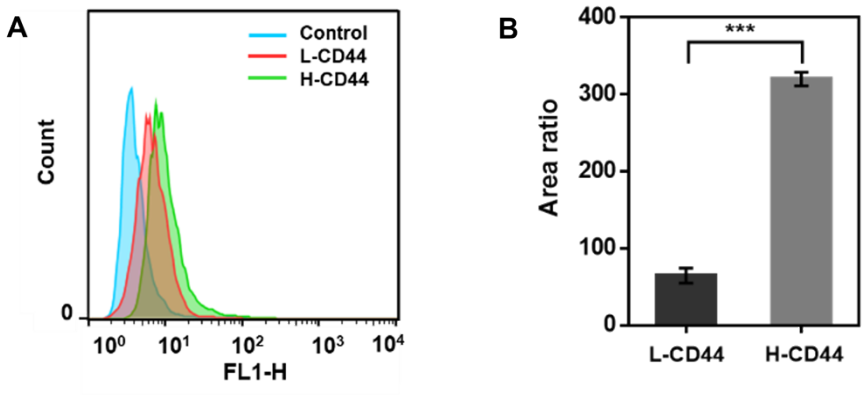


**Figure S14.** Detection of CD44 in the platelet samples from breast cancer patients with the lowest and highest CD44 expression by (A) flow cytometry and (B) mass-tagged MOF nanoprobe approach. Controls are the platelets that were not incubated with FITC-labeled CD44. L-CD44: platelets with lower expression of CD44, H-CD44: platelets with higher expression of CD44.

## 3. Supplementary Tables

**Table S1.** List of the DNA sequences used in this study. [a]

| | Name | Sequences (5′ to 3′) |
|---|---|---|
| Aptamer portion of the activable aptamer | TA6 | GAGATTCATCACGCGCATAGTCTTGGGACGGTGTTAAACGAAAGGGGACGACCGACTATGCGATGATGTCTTC |
| | TA61 | **GGTTGTGTGGTTGCAGTTGA**GAGATTCATCACGCGCATAGTCTTGGGACGGTGTTAAACGAAAGGGGACGACCGACTATGCGATGATGTCTTC |
| | TA62 | **GTGTGGTTGCAGTTGA**GAGATTCATCACGCGCATAGTCTTGGGACGGTGTTAAACGAAAGGGGACGACCGACTATGCGATGATGTCTTC |
| | TA63 | **TGGTTGCAGTTGA**GAGATTCATCACGCGCATAGTCTTGGGACGGTGTTAAACGAAAGGGGACGACCGACTATGCGATGATGTCTTC |
| Inhibitory DNA of the activable aptamer | INH1 | TACAATCTCTCAATTTT |
| | INH2 | TACAATCTCTCAACATTT |
| | INH3 | TACAATCTCTCAACTTTTT |
| | INH4 | TACAATCTCTCAACTGTTTT |
| | INH5 | TACAATCTCTCAACTGCTTTT |
| | INH6 | TACAATCTCTCAACTGCATTTT |
| | INH7 | TACAATCTCTCAACTGCAATTTT |
| | INH8 | TACAATCTCTCAACTGCAACTTTT |
| Competing DNA | C42 | GACTATGCGCGTGATGAATCTCTCAACTGCAACCACACAACC |
| Binding DNA | BDNA | AAAATGCAGTTGAGAGATTGTA |

[a] The sequences in bold represent the bases added at 5′ end of CD44 aptamer as the extended sequence.

**Table S2.** Comparison of our approach with the previously reported signal amplification methods for CD44 quantification.

| CD44 quantification methods | Linear range (ng/mL) | LOD (pg/mL) |
|---|---|---|
| **Fluorescence**[2] | $0 – 10^2$ | 23 |
| **Electrochemistry**[3] | $10^{-2} – 10^2$ | 10 |
| **Mass-tagged MOF nanoprobe** | $10^{-2} – 10^2$ | 5 |

**Table S3.** Evaluation of the accuracy and precision of the mass-tagged MOF nanoprobe approach.

| Concentration of CD44 | 10.0 pg/mL | 30.0 pg/mL | 1.00 ng/mL | 80.0 ng/mL |
|---|---|---|---|---|
| **Mean** | 9.28 | 27.9 | 1.05 | 80.5 |
| **%Bias** | -7.2 | -7.0 | 5.0 | 0.6 |
| **Intraday Precision (%CV)** | 0.9 | 9.9 | 9.3 | 5.8 |
| **Interday Precision (%CV)** | 6.6 | 14.5 | 10.0 | 11.6 |
| **n** | 18 | 18 | 18 | 18 |
| **Number of Runs** | 3 | 3 | 3 | 3 |

**Table S4.** Clinical information of normal individuals and breast cancer patients.

| Groups | Number | Female | Male | Age (SD) |
|---|---|---|---|---|
| **Breast cancer patients** | 54 | 54 | 0 | 50.3 (12.5) |
| **Normal individuals** | 10 | 6 | 4 | 76.2 (12.2) |

## 4. Supplementary Results

### 4.1. LC-MS/MS method of the mass tag

The AVLGVDPFR double-charged precursor ion 487.5 with three highly responsive product ions b2 *m/z* 170.9, y3 *m/z* 419.0 and y6 *m/z* 690.2 was selected for multiple reaction monitoring (MRM) transitions. The corresponding stable isotope-labeled peptide AV*LGV*DPFR with [D8] Val at positions 2 and 5 was synthesized as an internal standard. Thus, the peak areas of the MRM transitions (*m/z* 487.5 → *m/z* 170.9, *m/z* 487.5 → *m/z* 419.0, and *m/z* 487.5 → *m/z* 690.2) and the corresponding internal standard transitions were summed for the following quantitative analysis.

### 4.2. Characterization results of the mass-tagged MOF nanoprobe

First, TEM and SEM results revealed that the edges of PEG/mass tag@ZIF-8 MOF and BDNA/PEG/mass tag@ZIF-8 MOF were slightly blurred, whereas both ZIF-8 and mass tag@ZIF-8 MOF exhibited a regular rhombic dodecahedron shape.[4] This surface irregularity may be caused by the coating with PEG and BDNA.[5, 6] In addition, DLS results demonstrated that the average diameter of ZIF-8 MOF gradually increased from ~180 nm to ~210 nm with the sequential addition of the mass tag, PEG and BDNA. This result is consistent with the outcomes of TEM and SEM. Notably, by referring to the previous studies for optimization of MOF particle size, [7-10] we tuned molar ratio of $Zn(NO_3)_2 \cdot 6H_2O$ to 2-methylimidazole (1:8 to 1:640), reaction temperature (25 °C to 50 °C), reaction solvent ($H_2O$, MeOH and DMF) and reaction time (10 min to 8 h), and obtained the ZIF-8 MOF particles in the size range of 100 - 1000 nm. The results indicated that the ZIF-8 MOF with the particle size of 200 nm has a better stability and a higher carrying capacity of mass tags. The PXRD data confirmed that the modified ZIF-8 MOF retained the same crystalline form as the original material, suggesting that our modifications did not change the three-dimensionally ordered structure of ZIF-8 MOF.

Furthermore, the signal at 1677 $cm^{-1}$ in the FT-IR spectrum of the mass tag@ZIF-8 MOF corresponded to the C=O stretching mode of the mass tag. In the FT-

IR spectrum of PEG/mass tag@ZIF-8 MOF, a characteristic peak at 1114 $cm^{-1}$ corresponding to C–O–C appeared, indicating the presence of PEG. The peak approximately 1247 $cm^{-1}$ in the spectrum of BDNA/PEG/mass tag@ZIF-8 MOF, demonstrated the successful modification of BDNA. The signal intensity reduction at 1677 $cm^{-1}$ in the spectra of PEG/mass tag@ZIF-8 MOF and BDNA/PEG/mass tag@ZIF-8 MOF may be caused by the PEG coating, which also implied that the mass tag was encapsulated in ZIF-8 MOF rather than adsorbed on its surface.

Moreover, the zeta potential of BDNA/PEG/mass tag@ZIF-8 MOF was in a negative state, in contrast to that of PEG/mass tag@ZIF-8 MOF, further confirming the successful modification with BDNA. The energy dispersive EDX elemental mapping image showed the appearance of Zn, N, O, and P elements in the BDNA/PEG/mass tag@ZIF-8 MOF. In the TGA, a weight loss of 0.9% between 80 °C and 350 °C can be attributed to the mass tag. The weight loss of 4.2% between 350 °C and 430 °C can be ascribed to the decomposition of PEG molecules.

The dispersibility and stability of the BDNA/PEG/mass tag@ZIF-8 MOF nanoprobe were also investigated. Using visual observation and polymer dispersity index measurement (PDI), we found that the MOF nanoprobe maintained a good dispersion within 150 min at room temperature. Although part of the MOF nanoprobe settled due to gravity over time, it can be easily resuspended by gentle shaking. In addition, the stability of the MOF nanoprobe was assessed. As a result, the detected mass spectrometric signal was reduced to (91.5 ± 1.5)% after 1 week of nanoprobe storage.

Finally, to reduce steric hindrance effect, the amount of streptavidin-modified agarose beads used in this study was relatively higher than the amount routinely recommended for binding assays. The average number of MOF nanoprobe per streptavidin agarose bead was estimated to be no more than 20 for sample analysis.

### 4.3. Validation results of the mass-tagged MOF nanoprobe approach

The quality control (QC) results indicated acceptable accuracy and intra- and interday precision of the assay. In addition, the selectivity of the approach was

further evaluated. Remarkably, no significant signal was detected in the absence of C42 or CD44, and also in CD44-negative NIH-3T3 cells and CD44-blocked MDA-MB-231 cells, demonstrating good selectivity of the approach. Finally, the reproducibility of the approach was examined using five different lots of the nanoprobe. The results showed similar signal intensities with a relative standard deviation (RSD) of 2.1%. We also compared the assay with the other signal amplification methods previously reported, and a higher sensitivity was observed.

## References


1 A. Somasunderam, V. Thiviyanathan, T. Tanaka, X. Li, M. Neerathilingam and G. L. Lokesh, *Biochemistry*, 2010, **49**, 9106.

2 Y. Huang, X. Yao, R. Zhang, L. Ouyang, R. Jiang and X. Liu, *ACS Appl. Mater. Interfaces*, 2014, **6**, 19144.

3 R. Zhang, C. Rejeeth, W. Xu, C. Zhu, X. Liu, J. Wan, M. Jiang and K. Qian, *Anal. Chem.*, 2019, **91**, 7078.

4 J. Feng, X. Liang and Z. Ma, *Biosens. Bioelectron.*, 2021, **175**, 112853.

5 A. Maleki, M. A. Shahbazi, V. Alinezhad and H. A. Santos, *Adv. Healthc Mater.*, 2020, **9**, e2000248.

6 J. Zhang, M. He, C. Nie, M. He, Q. Pan and C. Liu, *Chem. Sci.*, 2020, **11**, 7092.

7 S. Watanabe, S. Ohsaki, T. Hanafusa, K. Takada, H. Tanaka, K. Mae and M. T. Miyahara, Chemical Engineering Journal, 2017, **313**, 724.

8 G. Lu, S. Li, Z. Guo, O. K. Farha, B. G. Hauser, X. Qi, Y. Wang, X. Wang, S. Han, X. Liu, J. S. DuChene, H. Zhang, Q. Zhang, X. Chen, J. Ma, S. C. Loo, W. D. Wei, Y. Yang, J. T. Hupp and F. Huo, Nat. Chem., 2012, **4**, 310.

9 Y. V. Kaneti, S. Dutta, M. S. A. Hossain, M. J. A. Shiddiky, K. L. Tung, F. K. Shieh, C. K. Tsung, K. C. Wu and Y. Yamauchi, Adv. Mater., 2017, **29**, 1700213.

10 R. Wu, T. Fan, J. Chen and Y. Li, ACS Sustainable Chemistry & Engineering, 2019, **7**, 3632.